ORIGINAL ARTICLE

Drug-Penetration Gradients Associated with Acquired Drug Resistance in Patients with Tuberculosis

Keertan Dheda[1,2*], Laura Lenders[1], Gesham Magombedze[3], Shashikant Srivastava[3], Prithvi Raj[4], Erland Arning[5], Paula Ashcraft[5], Teodoro Bottiglieri[5], Helen Wainwright[6], Timothy Pennel[7], Anthony Linegar[7], Loven Moodley[7], Anil Pooran[1], Jotam G. Pasipanodya[3], Frederick A. Sirgel[8], Paul D. van Helden[8], Edward Wakeland[4], Robin M. Warren[8], and Tawanda Gumbo[1,3*]

[1]Center for Lung Infection and Immunity, Division of Pulmonology and University of Cape Town Lung Institute, Department of Medicine, [2]Institute of Infectious Disease and Molecular Medicine, Faculty of Health Sciences, University of Cape Town, Cape Town, South Africa; [3]Center for Infectious Diseases Research and Experimental Therapeutics and [5]Institute of Metabolic Disease, Baylor Research Institute, Baylor University Medical Center, Dallas, Texas; [4]Department of Immunology, University of Texas Southwestern Medical Center, Dallas, Texas; [6]Department of Pathology and [7]Chris Barnard Division of Cardiothoracic Surgery, Department of Surgery, Groote Schuur Hospital and University of Cape Town, Cape Town, South Africa; [8]Division of Molecular Biology and Human Genetics, South African Medical Research Council Centre for Tuberculosis Research/Department of Science and Technology/National Research Foundation Centre of Excellence for Biomedical Tuberculosis Research, Stellenbosch University, Stellenbosch, South Africa

ORCID ID: 0000-0001-7592-8012 (T.G.).

Abstract

Rationale: Acquired resistance is an important driver of multidrug-resistant tuberculosis (TB), even with good treatment adherence. However, exactly what initiates the resistance and how it arises remain poorly understood.

Objectives: To identify the relationship between drug concentrations and drug susceptibility readouts (minimum inhibitory concentrations [MICs]) in the TB cavity.

Methods: We recruited patients with medically incurable TB who were undergoing therapeutic lung resection while on treatment with a cocktail of second-line anti-TB drugs. On the day of surgery, antibiotic concentrations were measured in the blood and at seven prespecified biopsy sites within each cavity. *Mycobacterium tuberculosis* was grown from each biopsy site, MICs of each drug identified, and whole-genome sequencing performed. Spearman correlation coefficients between drug concentration and MIC were calculated.

Measurements and Main Results: Fourteen patients treated for a median of 13 months (range, 5–31 mo) were recruited. MICs and drug resistance–associated single-nucleotide variants differed between the different geospatial locations within each cavity, and with pretreatment and serial sputum isolates, consistent with ongoing acquisition of resistance. However, pretreatment sputum MIC had an accuracy of only 49.48% in predicting cavitary MICs. There were large concentration–distance gradients for each antibiotic. The location-specific concentrations inversely correlated with MICs ($P < 0.05$) and therefore acquired resistance. Moreover, pharmacokinetic/pharmacodynamic exposures known to amplify drug-resistant subpopulations were encountered in all positions.

Conclusions: These data inform interventional strategies relevant to drug delivery, dosing, and diagnostics to prevent the development of acquired resistance. The role of high intracavitary penetration as a biomarker of antibiotic efficacy, when assessing new regimens, requires clarification.

Keywords: drug gradient; acquired drug resistance; sputum MIC; lung cavity; whole-genome sequencing

(Received in original form November 27, 2017; accepted in final form June 6, 2018)

*Contributed equally and cosupervised project.

Supported by Baylor Research Institute and the NIH (T.G.) and by the South African Medical Research Council, the European Developing Clinical Trials Partnership, the National Research Foundation, and the Oppenheimer Foundation (K.D.).

Author Contributions: K.D., L.L., and T.G. conceived of the research, designed the study, interpreted data, and wrote the draft of the manuscript; G.M. and T.G. developed and implemented the mathematical model; S.S., L.L., and A.P. performed the DNA extraction, curated the data, and interpreted the data; P.R. and E.W. performed whole-exome sequencing and *Mycobacterium tuberculosis* whole-genome sequencing; E.A., P.A., and T.B. developed and validated drug concentration assays and used the assays to measure tissue and blood drug concentrations; H.W. performed the dissection and measured cavity sizes and histological distances; K.D., L.L., and A.P. recruited the patients; T.P., A.L., and L.M. recruited the patients and performed the surgical resection; F.A.S., P.D.v.H., and R.M.W. performed the minimum inhibitory concentration work as well as a separate set of DNA extraction on *Mycobacterium tuberculosis*; J.G.P. performed statistical analyses; K.D. and T.G. are co–senior authors who directed the research; all authors wrote sections of the manuscript on the work they did.

Correspondence and requests for reprints should be addressed to Tawanda Gumbo, M.D., Center for Infectious Diseases Research and Experimental Therapeutics, Baylor Research Institute, Baylor University Medical Center, 3434 Live Oak Street, Dallas, TX 75204. E-mail: tawanda.gumbo@bswhealth.org.

This article has an online supplement, which is accessible from this issue's table of contents at www.atsjournals.org.

Am J Respir Crit Care Med Vol 198, Iss 9, pp 1208–1219, Nov 1, 2018
Copyright © 2018 by the American Thoracic Society
Originally Published in Press as DOI: 10.1164/rccm.201711-2333OC on June 7, 2018
Internet address: www.atsjournals.org

At a Glance Commentary

Scientific Knowledge on the Subject: There is evidence that tuberculosis (TB) drug penetration of human lung cavities is suboptimal, and it is widely accepted that most resistance arises in the TB cavity. However, how it arises and its relationship to drug levels has hitherto not been investigated. To our knowledge, this is the first study to evaluate how absolute drug levels vary at anatomically distinct locations across the human TB cavity and their relationship to phenotypic and genotypic susceptibility testing readouts.

What This Study Adds to the Field: Collectively, these data have implications for the prevention of acquired resistance and may explain the poor efficacy of conventional multidrug-resistant (MDR) TB regimens. A fundamental reappraisal may be required regarding: *1*) how anti-TB drugs and regimens are selected for clinical trials (focusing on drugs with high intracavitary penetration), *2*) how drugs are delivered to the diseased lung, and *3*) how drugs are dosed in individual patients to achieve high intracavitary concentrations. More comprehensive tests, such as deep sequencing, could be needed to detect micro-heteroresistance so that sputum readouts better approximate what is happening in the cavity. This will facilitate personalized medicine and individualized therapy to prevent resistance amplification in patients with MDR and or extensively drug resistant TB.

According to the United Nations, "antimicrobial resistance has become one of the biggest threats to global health and endangers other major priorities, such as human development" (1). A major component of this scourge is ascribable to multidrug-resistant (MDR), extensively drug resistant (XDR), and incurable tuberculosis (TB), which threaten to subvert the miracle of chemotherapy (2–4). X/MDR-TB is unsustainably costly to treat and is a threat to healthcare workers, and mortality rates are worse than many cancers (2–6). Acquired drug resistance (ADR) was first encountered as soon as chemotherapy was introduced, especially monotherapy, and has continued unabated (7–9). During MDR-TB treatment, ADR to quinolones and/or aminoglycosides is encountered in 9% to 14% of patients, after an average of 4.5 months of combination therapy (10, 11). Thus, ADR arises often, and quickly. The hope had been that directly observed therapy (DOTS) would eliminate ADR (7, 12, 13). Unfortunately, the problem of ADR is not circumvented even with high-quality DOTS (14). Recent evidence indicates that one common proximate cause of ADR is suboptimal antibiotic concentrations due to pharmacokinetic variability (15–18). Moreover, TB cavities are also a known major risk factor for ADR. Indeed, in patients with MDR-TB, cavities are associated with a fivefold risk of developing XDR while on DOTS (10, 11, 19, 20). However, what makes the lung cavity the cauldron where ADR is created, especially in the evolution from MDR-TB to either XDR or incurable TB?

In TB lung cavities (as we show in this report), antibiotics have to diffuse through a spherical volume of up to 1,000 cm^3 and traverse physicochemical barriers to reach high numbers of *Mycobacterium tuberculosis* (*Mtb*) organisms in the liquid-phase/caseum in the cavity center. These barriers could lead to variability in drug penetration. Indeed, the relative differential penetration of several drugs into TB lung cavities has been recently characterized, which may explain antibiotic sterilizing effect patterns (21, 22). Mathematical models have suggested that such antibiotic spatial heterogeneity, effectively resulting in monotherapy, could drive ADR in different bacteria, and this was specifically speculated to lead to ADR in TB (21, 23). However, no evidence has yet been offered to support this in TB, and the precise pharmacological explanations for ADR within the human TB cavity remain unknown. Here we caught *Mtb* resistance *in flagrante delicto* in its associations with antibiotic concentrations inside the human lung cavity.

Methods

Patient Recruitment and Dissection Procedures

In 2012 to 2013, we prospectively recruited patients referred to Groote Schuur hospital who had failed medical treatment and had been offered therapeutic surgical resection. The study was approved by the Human Research Ethics Committee of the University of Cape Town. Patients signed informed consent before all study tests.

On the day of surgery, antibiotics were administered under supervision and timed. In the operating room, a blood draw was performed simultaneous with the start of lung removal and placed on ice. Resected lung was immediately placed on ice and taken to the Biosafety Level 3 laboratory. Lung dissection procedures to avoid cross-contamination were undertaken by the pathologist, as described in the online supplement, including biopsy of tissue from seven different positions in the lung relative to the cavity (*see* Figure E1 in the online supplement). The biopsy from each position was used to culture *Mtb* and to measure drug concentrations. A buffy coat was also collected from each patient for whole-exome sequencing (WES) to characterize potential genes affecting drug pharmacokinetics.

Assays and Sequencing

WES for patients, and whole-genome sequencing (WGS) of *Mtb*, quality control, analyses, and SNP calls were performed as described in the online supplement. *Mtb* minimum inhibitory concentrations (MICs) were identified using the two standard assays, described in the online supplement. Measurement of drug concentrations used a multiplexed assay that we developed, as described in detail in the online supplement.

Pharmacokinetic/Pharmacodynamic Modeling of the Clinical Data

Pharmacokinetic modeling of each drug, at each position, was performed using ADAPT 5 software. We followed compartmental pharmacokinetic modeling steps described in prior work and in the online supplement (15, 24), from which we derived the 0- to 24-hour area under the concentration–time curve (AUC) and peak concentrations. The concentrations identified were then used to calculate the gradient, with serum as the reference concentration, because antibiotics will diffuse from blood vessels into the TB lesion.

AUC-to-MIC ratio, peak-to-MIC ratio, and percentage time concentration persists above MIC, or pharmacokinetic/pharmacodynamic exposures, have a direct relationship to both resistance suppression and amplification of resistant

subpopulations (15, 25–30). We calculated the AUC/MIC and peak/MIC at each cavity position. We also calculated the different intracellular pharmacokinetic/pharmacodynamic exposures of moxifloxacin, ethambutol, pyrazinamide, and isoniazid, on the basis of our prior studies (31, 32).

Sample Size Justification and Statistical Methods

A sample size of 14 patients allowed us to derive estimates with adequate power and confidence, as outlined in the online data supplement. We computed how different drug pharmacokinetic parameters were correlated with MIC at the different cavity locations using Pearson, Spearman, and Kendall methods. We also calculated how accurate sputum MICs were in predicting the MICs of the different isolates in the lung cavity in the same patient, on the basis of the formula for forecasting accuracy we have used in the past (33).

Results

Patient Clinical and Pharmacogenomic Features

We prospectively recruited 14 patients, whose TB histories and clinical features are shown in Table 1. Thirteen of the 14 (93%) patients had a documented prior history of TB treatments and had progressively acquired new drug resistance. All patients were receiving chemotherapy consisting of a cocktail of eight drugs: clofazimine, ethambutol, isoniazid, pyrazinamide, ethionamide, moxifloxacin, *para*-aminosalicylic acid (PAS), and terizidone (active moiety is cycloserine). Dosing was personalized, as shown in Table E1 in the online supplement. The most common antibiotic added to the eight was capreomycin (6 of 14, 43%) (Table E1). The patients had been on this therapy for a median of 13 months (range, 5–31 mo), and on DOTS, at the time of surgery.

Patient WES target enrichment was highly specific and efficient; about 70% of reads were on target and showed greater than 60 to 70 times average fold coverage. Nonsynonymous SNPs are summarized in the online supplement (Table E2) for the genes relevant to the cocktail of drugs patients were taking or had taken in the past. Table E3 shows the base substitutions in the relevant genes of each patient. Patients carried SNPs associated with either rapid metabolism or extensive transport of the antibiotics, consistent with pharmacokinetic variability as part of the events leading to the ADR.

Cavity Dissection and Drug Concentrations in Lung Cavities

The median (range) cavity diameter on the basis of caliper measurements was 4 cm (2–8 cm), and the volume of normal-appearing lung tissue plus the cavity biopsied covered a sphere of 382 cm^3 (180–1,150 cm^3). Human lung tissue from patients without TB was also spiked with known concentrations of each drug and then processed in a similar way to the TB cavity samples; the team members measuring drug concentrations were blinded to the existence of these samples. The concentrations in the spiked tissue were exactly as were spiked, which means that there was no degradation of drug due to the processing of the tissue.

The drug concentrations measured at each lung position are shown in Figure E2. The posttest results documenting the D-optimality–derived sampling time accuracy are shown in Figure E3. As described in detail in the online supplement, single time-point drug concentrations can accurately identify compartmental pharmacokinetic parameters and variances; we identified the serum pharmacokinetic parameter estimates shown in Table E4. The isoniazid, ethambutol, pyrazinamide, and terizidone pharmacokinetic parameter estimates were in the range of those we have identified with intensive pharmacokinetic sampling

Table 1. Clinical Features and Tuberculosis Treatment History in 14 Patients with Tuberculosis

Sex	Age (*yr*)	TB Disease History (yr before Surgery)*	Lung Cavities	TB Diagnosis at Time of Surgery	Drugs Added to 8-Drug Core Regimen
Female	14	MDR (2), XDR (1)	1	XDR-TB	Amoxicillin-clavulanate 500 mg/125 mg twice daily Capreomycin 1,000 mg 3 times per week
Female	24	Susceptible TB (3), MDR (2), XDR (0.5)	3	XDR-TB	—
Female	33	Susceptible TB (5), MDR (4)	2	MDR-TB	Capreomycin 1,000 mg daily
Male	29	Susceptible TB (9), MDR (7), XDR (3)	2	XDR-TB	Capreomycin 750 mg daily Clarithromycin 500 mg daily
Male	41	XDR (6)	2	XDR-TB	Amikacin 1,000 mg daily
Male	23	MDR (3), pre-XDR (3), XDR (1)	1	XDR-TB	Clarithromycin 500 mg daily
Female	26	MDR (3), XDR (1)	2	XDR-TB	Capreomycin 1,000 mg daily Clarithromycin 500 mg daily
Female†	40	MDR (4), pre-XDR (0.5)	1	Pre-XDR	—
Male	29	Susceptible TB (4), MDR (2), XDR (1)	1	MDR-TB	Capreomycin 1,000 mg daily
Female	16	Susceptible TB (4), MDR (3), XDR (2)	1	XDR-TB	Linezolid 600 mg daily
Female	49	MDR-TB (1), XDR (0.5)	1	XDR-TB	—
Female	50	Susceptible TB (8), XDR (2)	1	XDR-TB	Capreomycin 1000 mg daily
Female†	42	No previous TB history	2	XDR-TB	—
Female	48	Susceptible TB (1.5), XDR (1)	2	XDR-TB	—

Definition of abbreviations: MDR = multidrug resistant; TB = tuberculosis; XDR = extensively drug resistant.
*How long patient was diagnosed with disease.
†HIV coinfection and on antiretroviral therapy.

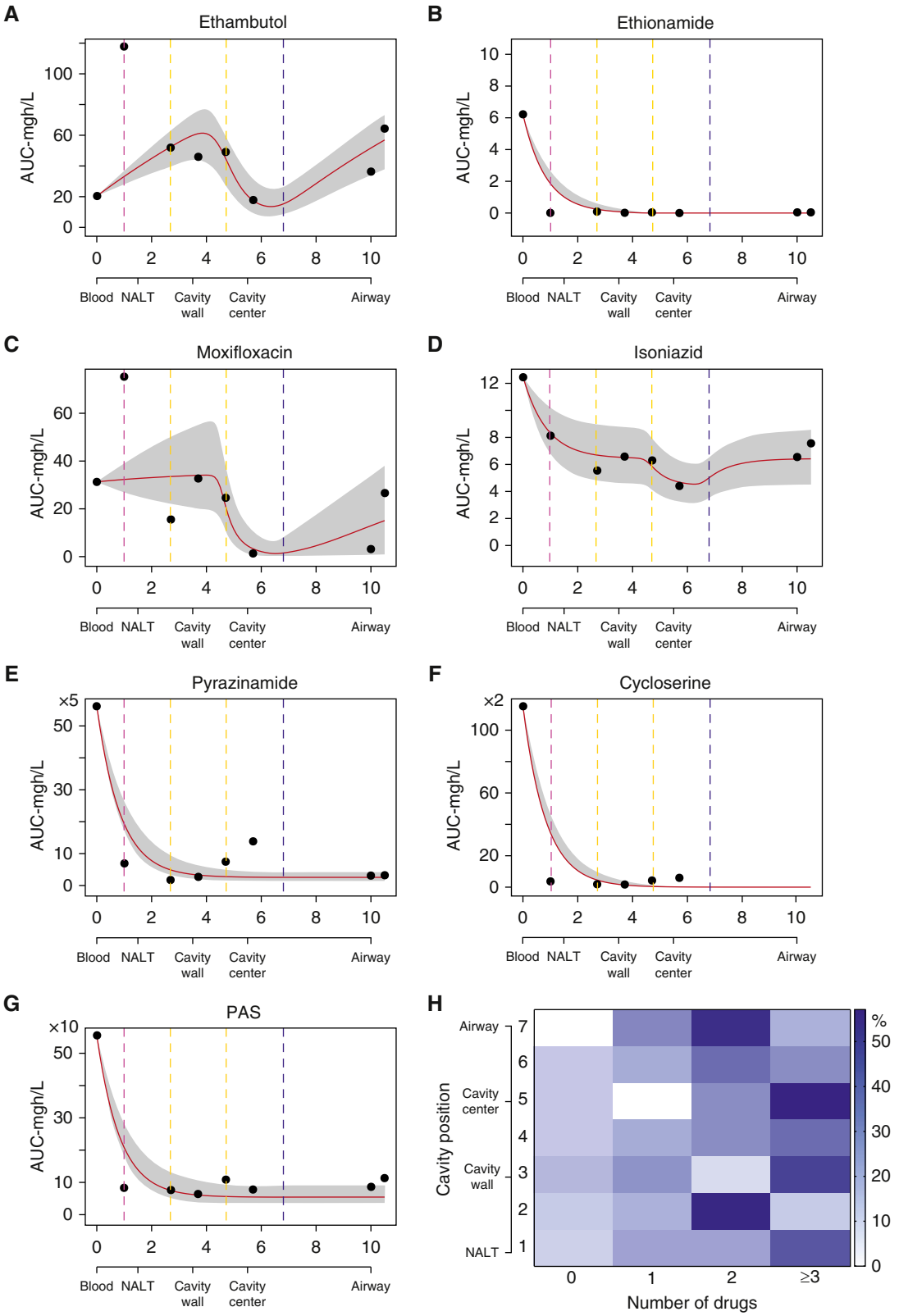

Figure 1. Number of drugs and concentration gradient in a dynamical sink model. (*A–G*) Data points (circles) are mean area under the concentration–time curve (AUC) values at that cavity position, and the shaded area indicates 95% confidence intervals fitting to a dynamical sink model. The *x*-axis is distance in centimeters; we also include a description of cavity position on each *x*-axis. The colored vertical lines mark transition zones/boundaries between adjacent histopathological regions on the second *x*-axis. The *y*-axis is the 0- to 24-hour AUC in mg · h/L. For (*A*) ethambutol, (*C*) moxifloxacin, and (*D*)

schedules in the general Western Cape TB population in the past (15, 24, 34), which means that even with the single time-point sampling, the pharmacokinetic modeling identified precise clearances and volumes of distribution. The drug clearances in Table E4 were on the higher end of the distribution for these prior study populations, consistent with drug metabolism SNPs identified in Tables E2 and E3.

Scatter plots of AUC versus cavity distance and position ratios at these points revealed that the lowest concentrations were most commonly encountered in the cavity center or the air–caseum interface, mathematically reminiscent of dynamical sinks (35). Therefore, we modeled the AUCs versus distance in centimeters (with serum designated 0 cm) using the dynamical sink model detailed in the online supplement, which revealed the results shown in Figures 1A–1G. Figure 1 shows that model fits for moxifloxacin and isoniazid demonstrated the potential well of the sink at around 6 cm, which is at the air–caseum interface, consistent with steep decline in drug diffusion across the fibrotic cavity wall and the air–caseum interface. Ethambutol had a similar shape, but in all cavity positions ethambutol concentration was higher than in serum. The increases in concentration of these drugs in the airways (second shoulder) could reflect a second drug diffusion direction and source, likely from the bronchial arterial circulation. For ethionamide, PAS, pyrazinamide, and cycloserine, Figure 1 shows a second decline pattern, a steep but smooth decline in the first 1 to 2 cm and before the cavity wall. Clofazimine is not shown because the concentrations in the cavity were below limits of quantitation in our assay, except in one patient, and represent an extreme example of reduced penetration. The clofazimine could still be detected inside cavities of 5 of 14 patients and was thus above limits of detection of 0.31 mg/L but below limits of quantitation.

The mean number of drugs (percentage coefficient of variation) detected at each lung cavity position was 3.0 (59.0%), whereas those above lower limit of quantitation were 2.8 (64.8%) (drugs shown in Figure E4).The mean number of drugs with effective concentrations above the lowest MIC in epidemiologic study distributions reported in the literature fell to 2.1 (70.6%) drugs ($P < 0.01$), shown by cavity position in Figure 1H (24, 30, 36–38). Because all patients were receiving at least eight drugs, this means that penetration into the cavity was highly variable. Only 19 (21%) of the different cavity positions had effective monotherapy, at the most, which means that in the majority of positions mechanisms other than monotherapy better explained ADR.

MICs of Different Antibiotics by Cavity Geospatial Location

MIC results were the same on two separate occasions and, as shown in Figures 2A–2F, are arranged by cavity position. The MICs for different drugs differed between the sputum and the different lung positions, which means that MICs were geospatially constrained. Uniquely, isolates in the same cavity would have MICs above critical concentration, indicating resistance, whereas those from other positions in the same cavity were drug susceptible. This means that the *Mtb* was still in the process of developing ADR, consistent with patient history. The MICs of isoniazid, rifampicin, pyrazinamide, and kanamycin were all at or above the highest concentration we used in the assay. Conversely, all linezolid and clofazimine MICs were at less than or equal to 0.5 mg/L, which is the lowest concentration tested in the assay.

Given that MICs were geospatially constrained, we calculated how accurate contemporaneous sputum isolates' MICs were in predicting the MICs at the lung cavity positions in the same patient, which revealed results shown in Figure 2G. These isolates derived from sputum and cavity samples were contemporaneously collected at the time of surgery and are distinct from serial isolates collected before and during the course of treatment in seven patients. The lowest accuracy was for moxifloxacin sputum MICs, which was 30.56% (95% confidence interval [CI], 5.14–55.97%), and the highest predictive accuracy was for amikacin MICs, which was 95.56% (95% CI, 90.18–100.90%). However, the high predictive accuracy for amikacin was an outlier and artifactual: 47 of 63 (75%) MIC values greater than or equal to 16 mg/L, which was the highest amikacin concentration tested in the assay. Overall, the accuracy was 54.6 (95% CI, 47.6–61.6) if all MICs were included, and 49.48% (95% CI, 52.51–79.71%) when amikacin MICs were excluded. Figure 2H is a sensitivity analysis in which all results with a one-tube dilution difference in MIC compared with sputum MIC were excluded from the analysis; the predictive accuracy was 55.46% (95% CI, 47.20–63.74%). If, on the other hand, the one-tube dilution difference with sputum was considered an identical MIC value, then the predictive accuracy was 61.76% (95% CI, 54.63–68.89%). Thus, the accuracy did not change much regardless of assumption changes, and the sputum MICs remained poor predictors of drug susceptibilities of isolates in lung cavities.

The Relationship between MIC and Location-Specific Concentration Heterogeneity

Each progressively higher MIC makes it increasingly more difficult to achieve bactericidal and sterilizing effect and indicates more resistant bacteria; we defined ADR as an increase in the MIC to values above specific critical concentrations (15, 24–30). Thus, MIC values are a *sine qua non* of resistance (15, 24–30, 36, 39–42). The correlation coefficients between MIC (and hence degree of resistance) and different drug concentration measures are shown in Figure 3. We examined Pearson, Kendal tau, and Spearman correlations: all three showed similar results. There were statistically significant and high negative correlations between moxifloxacin,

Figure 1. (Continued). isoniazid, the potential "well" of the sink is at the air–caseum interface (marked "cavity center" in figure), and the shape suggests two directions of diffusion from outside the cavity and also directly into airways. For (*B*) ethionamide, (*E*) pyrazinamide, (*F*) cycloserine, and (*G*) *para*-aminosalicylic acid (PAS), there is steep decline, consistent with concentration declining inversely proportional to an exponent of the distance from the source. (*H*) Heat map showing the effective number of drugs at each location. The percentage of patients with the number of drugs at each position is shown by shades of blue (scale); as an example, in position 7 (airway) 50% of patients had two effective drugs (deep blue). The heat map shows the heterogeneity in drug penetration into each geospatial location. The number of effective drugs by cavity position using each of the three definitions is shown in Figure E4. NALT = normal-appearing lung tissue.

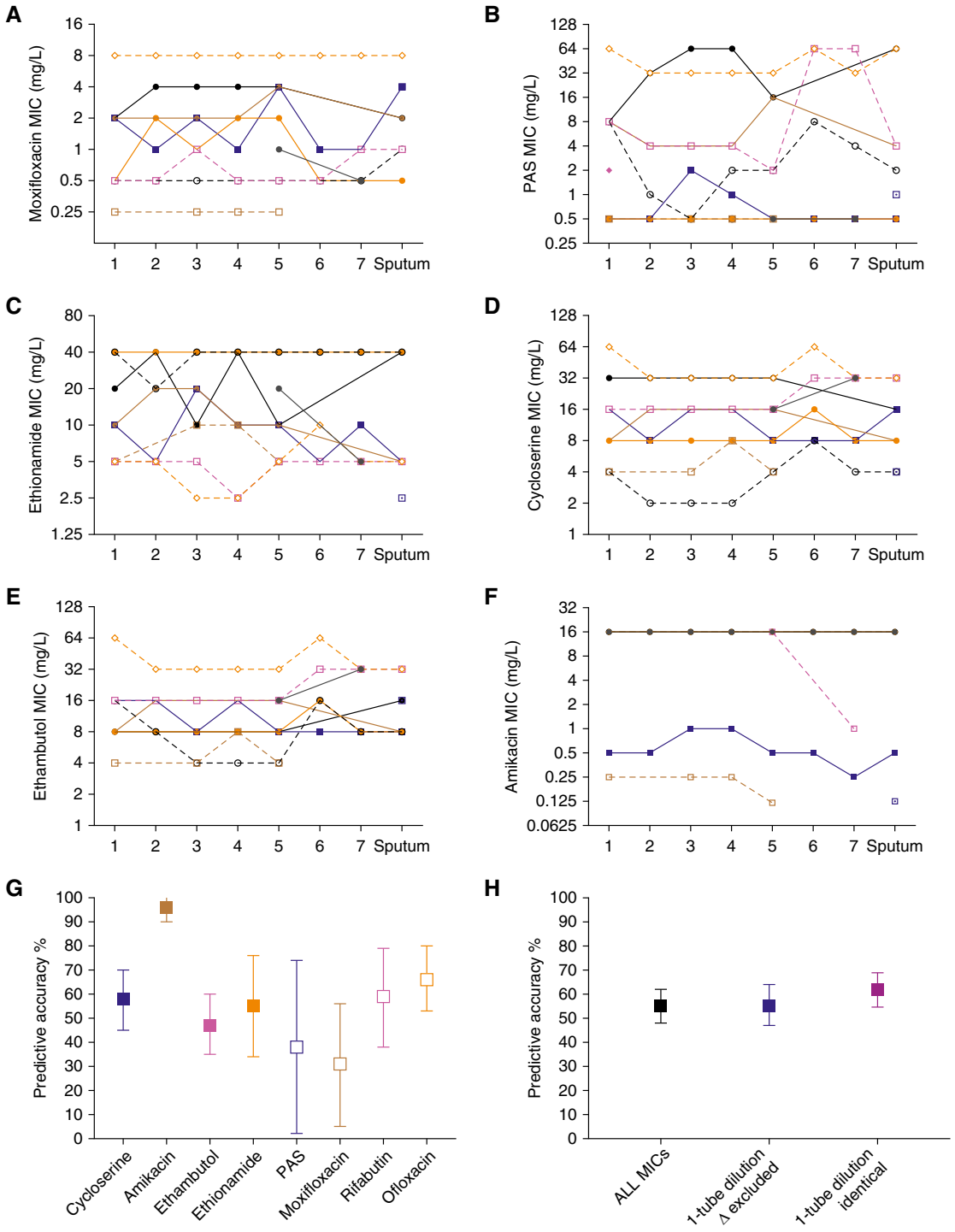

Figure 2. Minimum inhibitory concentration (MIC) in sputum and by cavity position. (*A–F*) MICs of isolates from each patient are joined by a line to allow easy tracing across the tuberculosis cavity. Some of the lines for different patients overlapped. There were differences in MIC by greater than one-tube dilution in many instances. If standard critical concentrations are used to categorize "resistant" from "susceptible," it can be seen for that for (*A*) moxifloxacin (0.5 or 2.0 mg/L), (*B*) *para*-aminosalicylic acid (PAS) (2.0 mg/L), (*C*) ethionamide (5.0 mg/L), (*D*) cycloserine (10/40 mg/L), (*E*) ethambutol (5.0/10 mg/L), and (*F*) amikacin (4.0 mg/L), there was a considerable proportion of patients with both drug-susceptible and drug-resistant isolates at the same time. (*G* and *H*) The square indicates the mean estimates, and bars indicate 95% confidence intervals. For each drug, we examined how accurate the sputum MIC value was in predicting the MIC of *Mycobacterium tuberculosis* isolates inside that patient's single cavity. We tested isolates in one cavity from each patient, although most patients had more than one cavity.

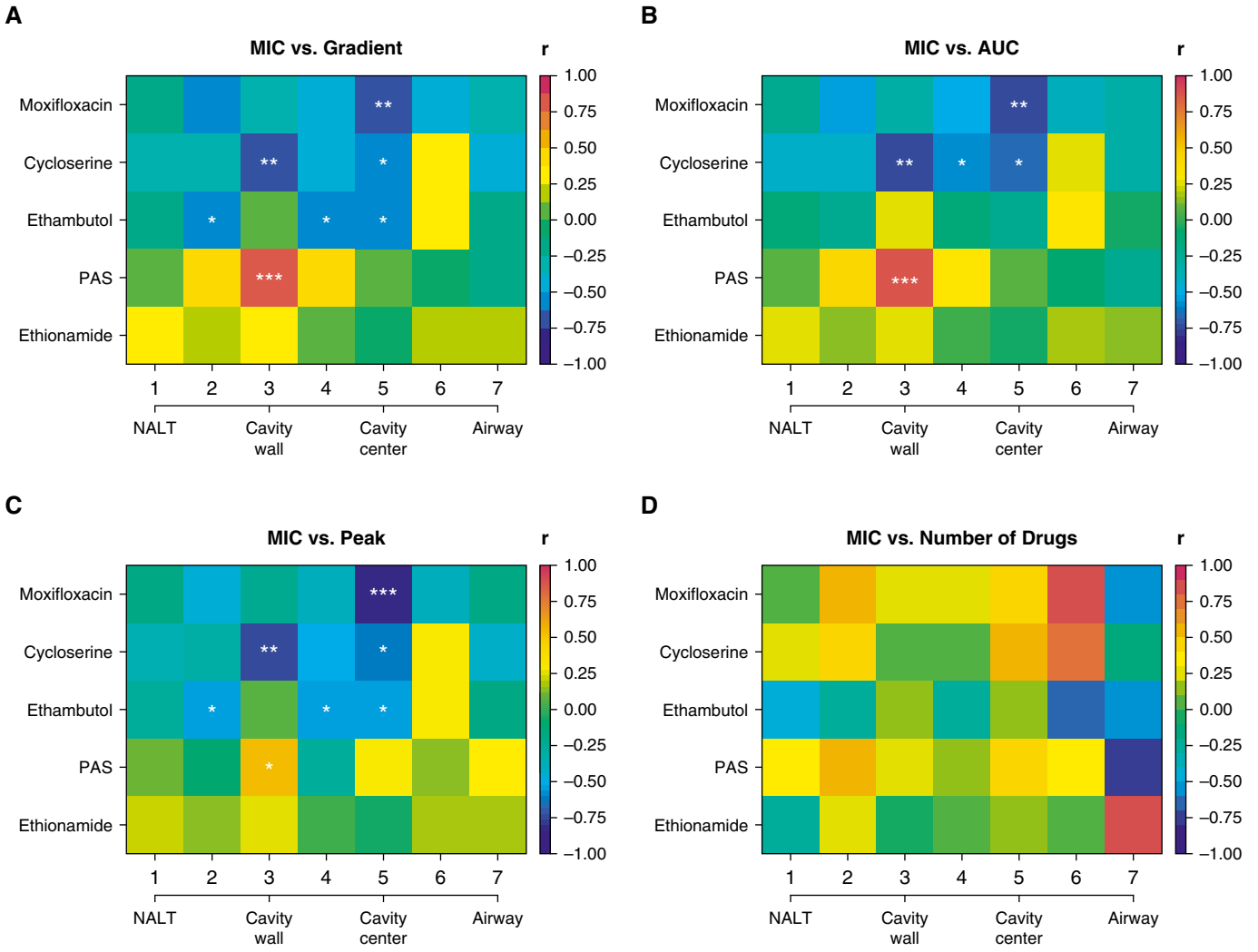

Figure 3. Correlation of minimum inhibitory concentration (MIC) with drug parameters by cavity geospatial position. The cavity center denotes the air–caseum interface. We examined for both Pearson and Spearman correlations, as well as the Kendall tau. Results are for Spearman *r*. *P* values are encoded as not significant if ⩾0.05. **P* < 0.05, ***P* < 0.01, and ****P* < 0.001. (*A*) The relationship of MIC to gradient, in this case expressed as the ratio of area under the concentration–time curve (AUC) at the cavity position to the AUC in the blood, shows a moderate to high negative correlation with MIC (i.e., darker blue) for all drugs except ethionamide and in several positions for *para*-aminosalicylic acid (PAS). For PAS, the significant *P* values are for a positive correlation between MIC and concentration. (*B*) The relationship between actual 0- to 24-hour AUC (mg · h/L) and MIC shows strong negative *r* for the drugs, except for PAS. (*C*) Similar findings are noted when peak concentration was used as drug concentration. These negative correlations shown in *A*–*C* indicate that high MIC (drug resistance) was associated with low drug levels (gradient, peak, and/or AUC). (*D*) Shows complex correlation patterns for number of drugs versus MIC. In general, the correlation between number of drugs and MIC was low, and no position had correlation associated with a $P < 0.05$. This means, surprisingly, that spatial monotherapy, or even dual therapy, was the least strongly correlated with acquired drug resistance, likely because eight or more drugs were administered. NALT = normal-appearing lung tissue.

ethambutol, or cycloserine MICs versus concentrations in a number of cavity positions (Figures 3A–3C). In other words, low drug concentrations at a position were associated with higher MICs. For ethambutol and moxifloxacin, peak concentrations had higher correlation coefficients with MICs than did AUC, whereas for cycloserine it was the opposite. A very informative situation was encountered with clofazimine and linezolid. Only one patient was receiving linezolid treatment, and thus *Mtb* isolates in patients' cavities had not been exposed to the drug before surgery. Consistent with that, linezolid MICs were less than or equal to 0.5 mg/L in all cavity isolates, indicating no resistance. Similarly, the clofazimine MICs were less than or equal to 0.5 mg/L in all isolates, as if the isolates had not been exposed to the clofazimine despite months of therapy, consistent with our finding of below limits of quantitation clofazimine concentrations inside cavities.

Finally, we examined the relationship between the number of drugs at each cavity location to MICs, with results shown in Figure 3D. The most common drug encountered as monotherapy was ethambutol, at 13 of 19 (68.42%) geospatial

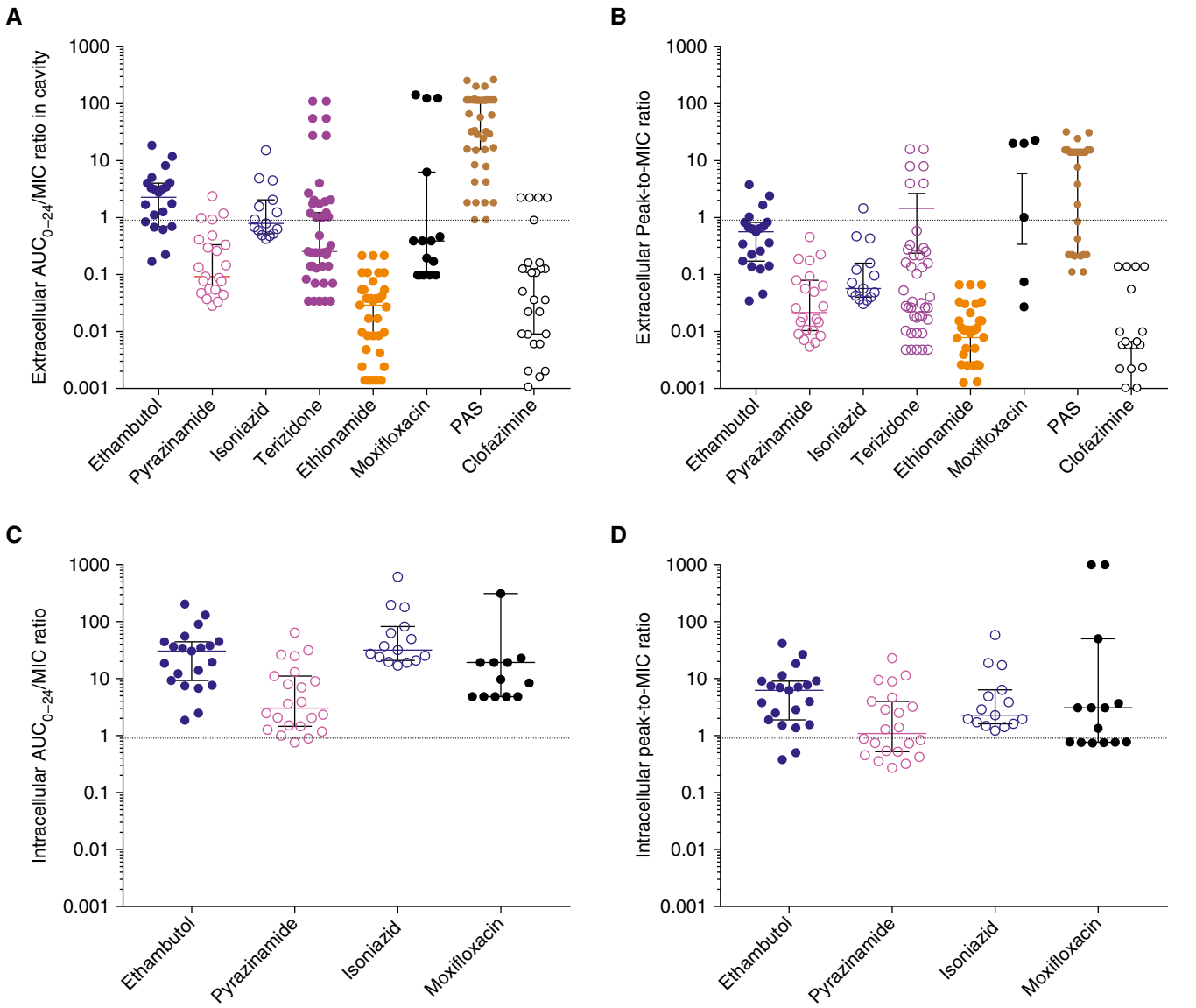

Figure 4. Pharmacodynamic exposures achieved inside tuberculosis cavities. Exposure ratios were derived from the measured area under the concentration–time curve (AUC) and minimum inhibitory concentration (MIC) matched by biopsy position; extracellular and intracellular exposures were calculated for each position. In prior studies, the free drug exposures associated with resistance amplification were an ethambutol peak/MIC of less than 49 and $AUC_{0–24}$/MIC < 272, a pyrazinamide percentage time above MIC < 67%, which translates to a peak/MIC < 2.5, or an $AUC_{0–24}$/MIC < 43, an isoniazid peak/MIC < 150 and an $AUC_{0–24}$/MIC < 700, and a moxifloxacin $AUC_{0–24}$/MIC < 106 (25–27, 29). (*A*) For the extracellular AUC/MIC ratios, the proportions of positions with exposures that have been demonstrated to amplify the population of drug-resistant mutants in the hollow fiber system model of tuberculosis were 100% for ethambutol, 100% for pyrazinamide, and 100% for isoniazid, but 80% for moxifloxacin. The hatched line indicates exposures above and below a ratio of 1. Although the resistance amplification ratios for the rest of the drugs are unknown, the median $AUC_{0–24}$/MIC values of clofazimine (0.05), ethionamide (0.03), and cycloserine (terizidone, 0.25) mean that most values were below the MIC, except for *para*-aminosalicylic acid (PAS). (*B*) On the basis of the extracellular peak/MIC ratios, the proportions of positions with exposures that amplify drug-resistant subpopulations were 100% for all drugs. The median peak/MIC ratios for ethionamide (ratio = 0.008), cycloserine (ratio = 0.033), and clofazimine (ratio = 0.002) mean that these drugs had more peak concentrations below MIC, with the exception of PAS (ratio = 14). (*C*) Because of intracellular accumulation of the drugs, the AUC/MICs were in the resistance amplification range for 100% for ethambutol and isoniazid, 98% for pyrazinamide, and 73% for moxifloxacin. (*D*) For intracellular peak/MIC ratios, all ethambutol and isoniazid exposures were in the resistance amplification range, but for only 59% of pyrazinamide.

monotherapy locations. Figure 3D shows that ethambutol showed the strongest negative correlation with MIC; however, the *P* values for the number of drugs did not reach statistical significance in any position, suggesting that spatial monotherapy was not associated with MICs. The same lack of statistical significance held true when the number of drugs was defined as either any detectable drugs or as those above the limits of quantitation.

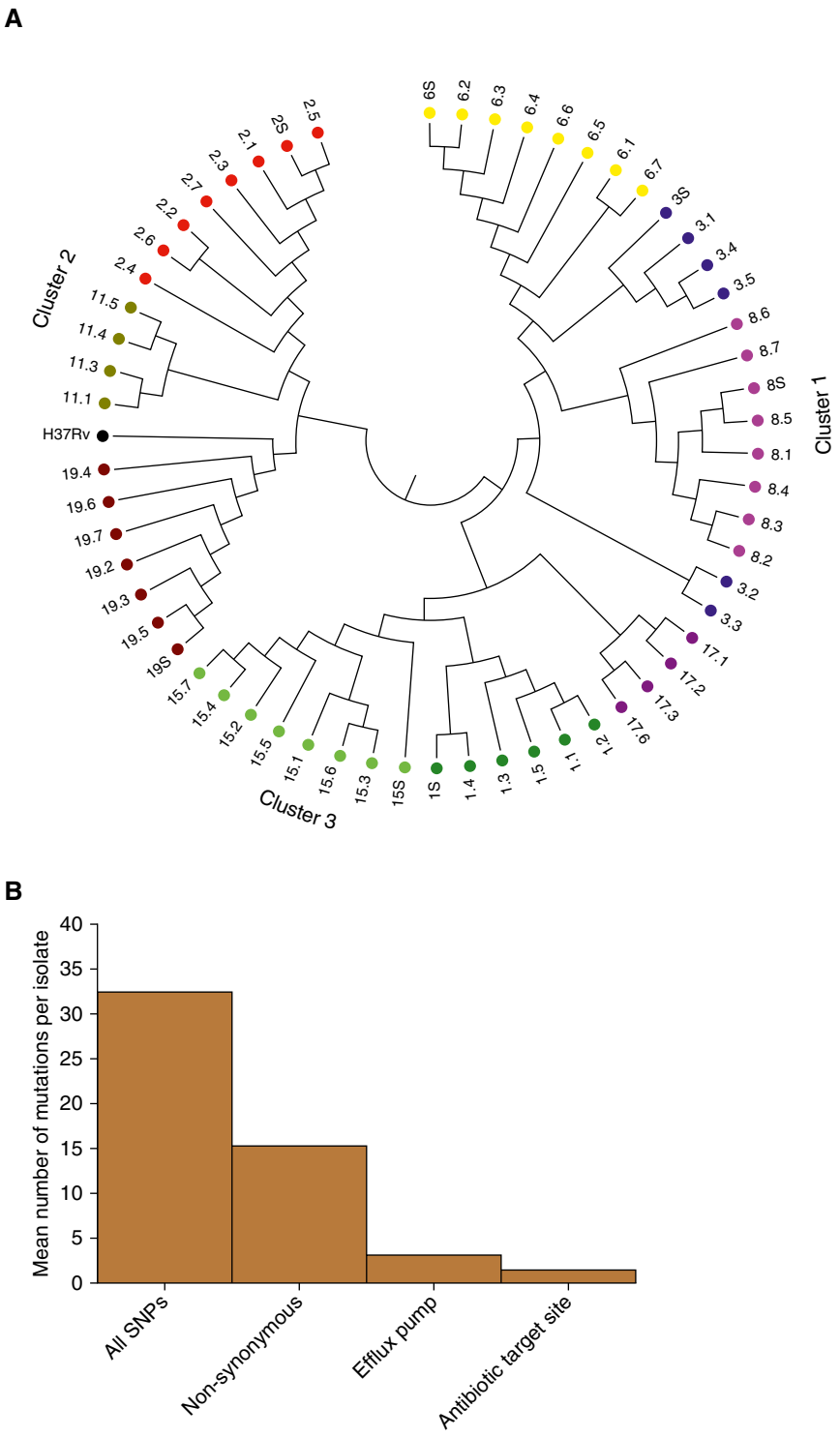

Figure 5. Whole-genome sequencing (WGS)-based variants in sputum and cavitary bacterial isolates. (*A*) WGS-based diversity of isolates revealed heterogeneity within each cavity, from patients who had more than two cavitary isolates that passed WGS quality control. Each color code indicates patient designation (also numbered), and the number (0.1, 0.2, 0.3, 0.4, 0.5, 0.6, 0.7, or S [sputum]) after the decimal indicates cavity positions specified in Figure E1. There were three clusters by relatedness and genetic distance; we give the position of the reference *Mycobacterium tuberculosis* H37Rv strain for context. As an example, sputum isolate 19.S differed from the neighbor 19.5 by 6 SNPs, shown by the bar height in the dendogram, whereas on the other extreme, 19.4 differed from

Drug Exposures Achieved Inside Pulmonary Cavities

Figure 4A shows that the mean AUC/MIC ratio for isoniazid (2.3 ± 3.8), ethambutol (3.5 ± 4.4), pyrazinamide (0.4 ± 0.6), and moxifloxacin (27 ± 54) among extracellular bacteria were all in the exact range associated with amplification of resistant subpopulations (25–29, 40). Similarly, peak/MIC ratios shown in Figure 4B were in the range associated with resistance amplification. Although PAS, clofazimine, ethionamide, and cycloserine exposures associated with resistance amplification are unknown, for ethionamide, cycloserine, and clofazimine most peak/MIC ratios were less than 1 and would thus not kill *Mtb* and likely only amplify resistance. Figures 4C and 4D show that the mean intracellular AUC/MIC exposures for isoniazid (94 ± 155) and ethambutol (40 ± 49) were still in the range associated with amplification of resistant subpopulations (25–29, 40). However, for intracellular moxifloxacin (AUC/MIC = 1,273 ± 2,611) and pyrazinamide (peak/MIC = 3.6 ± 5.4), 27% and 41% of exposures were above the resistance suppression thresholds, respectively (25–29, 40).

Mtb WGS and ADR

The cavitary and sputum *Mtb* isolates underwent WGS twice at two different research centers in two separate extractions, each using freshly prepared libraries. The call rates between the two centers are shown in Table E5. A total of 3,035 very high-quality common variants were called (call rate ⩾ 95%) and used in further analyses: 2,806 were SNPs. The median number of SNPs per cavity was 37 (range, 18–165), which was 5.2 (range, 3.1–28) SNPs per biopsy position. Hierarchical clustering revealed results shown in Figure 5A, which demonstrates considerable isolate heterogeneity within each cavity and the contemporaneous sputum isolate at time of surgery, consistent with MIC heterogeneity within each cavity and ongoing ADR.

In seven of the patients we had collected sputum isolates pretreatment (i.e., ∼24 to 48 mo before surgery and at time points thereafter), designated as $t = 0$, which we compared with WGS of isolates from sputum and cavities at $t = 1$ (i.e., at time of surgery) within each patient. This enabled us to interrogate the evolution of

resistance over time using serial isolates from the respiratory tract in individual patients. The comparative results are shown Figure 5B and in Table E6. Figure 5B shows the number of new nonsynonymous SNPs per isolate at $t = 1$ not present at $t = 0$. Table E6 is an Excel document with three sheets characterizing the SNPs in detail. The first sheet lists all new SNPs at $t = 1$ that developed since $t = 0$ in isolates from the same patient. The second sheet lists all validated *Mtb* genes known to be associated with antibiotic resistance and efflux pumps, which we used to query all the SNPs. The results of the query of drug-resistance–associated SNPs (*see* third Excel sheet in Table E6) at $t = 1$ not present at $t = 0$ (pretherapy isolate) in the same patient are shown in Figure 5B. Table E5 shows that the new antibiotic resistance SNPs were often encountered at some cavity positions and not others at the time of surgery, further suggesting that the process of ADR was not yet complete and was ongoing.

Discussion

In this prospective study, we documented ADR by: *1*) patient history; *2*) MIC heterogeneity within cavities, such that at some positions MICs indicated resistance and at some they indicated susceptible isolates within the same cavity; and *3*) new drug-resistance–associated SNPs in *Mtb* isolates on treatment with a cocktail of antibiotics for at least 5 months and not present at a time point before treatment. Mathematical models that depend on the concept of spatial monotherapy, and the generation and migration of drug-resistant clones against a concentration gradient, have been proposed to explain ADR (21, 23, 43, 44). Our dynamical sink model of distance dependence revealed two patterns of drug concentration decline. The first was a "well" at the air–caseum interface due to a steep fall at the fibrous cavity wall and in the fluid-like caseum phase. The second was a concentration decline inversely proportional to the distance from the source. These two patterns, and their variability, had two major consequences. In the majority of locations, we observed AUC/MIC and peak/MIC exposures known to amplify ADR subpopulations for isoniazid, ethambutol, pyrazinamide, and moxifloxacin. Second, we also found that MICs were inversely associated with gradient, peak concentration, and AUC. On the other hand, spatial monotherapy was not statistically associated with increased MIC and was encountered in only a minority of positions, and the presence of two to three drugs at effective concentrations was the most common scenario. We propose that the two former scenarios could be more important than spatial monotherapy in development of *Mtb* ADR from MDR-TB to XDR in the face of more than eight-drug therapy.

There are several possible direct clinical implications of our findings. First, the results imply that fundamental changes may be required to the way in which anti-TB drugs and regimens are selected for clinical trials (focusing on drugs with high intracavitary penetration), delivered to the site of disease, dosed in individual patients, and monitored during therapy. Inhaled formulations as therapeutic adjuncts to oral therapy, to overcome the low concentrations in the cavity center for most of the drugs studied (Figure 1), could be needed. However, in some patients, inhalational therapy will be limited by poor ventilation in the lung regions with large cavities (45). For other drugs, such as moxifloxacin, there may be need for increased doses to achieve AUC/MIC and peak/MIC ratios higher than currently achieved and, for others, strategies such as therapeutic drug monitoring to minimize ADR and the emergence of incurable TB (2, 3). Second, our drug penetration results may also have implications for explaining the ~50% treatment success rate using the conventional World Health Organization–approved MDR-TB regimen and the recent suboptimal results of the "Bangladesh-like MDR-TB regimen" evaluated in the STREAM 1 (Stage 1 of the Evaluation of a Standard Treatment Regimen of Anti-tuberculosis Drugs for Patients with MDR-TB) study, which includes moxifloxacin, clofazimine, pyrazinamide, isoniazid, and ethambutol (among others) that we studied here, as well as disappointing clofazimine results from China (46). Several of these drugs had poor penetration of lung cavities. Thus, there is likely a need to find drugs that have better penetration into TB cavities. A third important finding involves use of sputum cultures to individualize drug choice and drug doses in patients with MDR-TB. Is a predictive accuracy of only 50% regarding MICs in sputum isolates good enough to change therapy targeting intracavitary isolates? This could be explained by within-subject purifying mutations arising *de novo* within patients, as recently described in autopsy studies of disseminated TB in patients with AIDS (47). Regardless, findings of the spatial MIC heterogeneity present a special conundrum to clinical decision making in treatment of patients with MDR and XDR-TB and their exposed contacts.

There are several limitations. Our patients had been receiving treatment for 13 months for the current episode, on average, and had a history of prior TB for an average of 3 years, which means they likely had end-stage cavities and thickened cavity walls. It is unclear if the same drug penetration findings would be generalizable to newly diagnosed patients' cavities with thin walls or to those with drug-susceptible TB. However, the same relationships between drug concentration and ADR have been identified in preclinical models of drug-susceptible TB with first-line anti-TB drugs and quinolones (17, 25–27, 29). Second, we calculated caseum/serum ratios of 0.48 ± 0.16 for pyrazinamide and 3.09 ± 1.91 for moxifloxacin from the publication by Prideaux and colleagues (21). The average measured caseum/serum concentration ratio was 0.45 for pyrazinamide in our patients, and our dynamical sink model revealed

Figure 5. (Continued). 19.6 by 25 SNPs in the largest height for isolates in patient 19, within the same cavity. This shows much diversity of SNPs in each cavity; for the cavity in patient 3 (blue), there were two completely unrelated strains of different phylogenetic lineage. (*B*) *y*-axis shows the mean number of new mutations in the $t = 1$ isolate versus $t = 0$ isolate. Isolates from patients who had WGS of isolates before the current treatment episode ($t = 0$; time of diagnosis) revealed new nonsynonymous mutations compared with the time of lung explant or current treatment at $t = 1$. The mean number of SNPs in drug-resistance–associated genes (target site and efflux pumps) in the seven sets of isolates is for nonsynonymous mutations. Genes with new target site mutations included *gyrA* (quinolone resistance) and *gidB* (aminoglycoside resistance), consistent with evolution from multidrug-resistant tuberculosis before current treatment episode to extensively drug-resistant tuberculosis after ~5 months of therapy.

moxifloxacin accumulation in the cavity wall. These two factors suggest that the drug penetration factors we identified will be similar across different spectra of patients. In the Kramnik mouse model of drug-susceptible TB, where mice with new necrotic granulomas with a fibrous capsule were treated, there were higher numbers of drug-resistant *Mtb* inside hypoxic encapsulated granulomas compared with cultures from nonnecrotic TB lesions (20). Thus, it is likely not age of lesion that is important, but the tissue architecture of the lesion. Patients with any cavitary disease should thus have drug doses optimized and be treated with drugs that are better able penetrate cavities.

In conclusion, a drug-penetration gradient across the TB cavity wall in patients with MDR-TB likely creates two scenarios associated with acquisition of resistance: antibiotic exposures that amplify ADR and low drug concentrations that drive up MICs. Interventional strategies to prevent the development of drug-resistant TB will involve reversing these scenarios. ■

Author disclosures are available with the text of this article at www.atsjournals.org.

References

1. World Health Organization. United Nations high-level meeting on antimicrobial resistance. Geneva: World Health Organization, 2016 [accessed 2017 Nov 27]. Available from: http://www.un.org/pga/71/2016/09/21/press-release-hl-meeting-on-antimicrobial-resistance/.
2. Dheda K, Gumbo T, Maartens G, Dooley KE, McNerney R, Murray M, *et al*. The epidemiology, pathogenesis, transmission, diagnosis, and management of multidrug-resistant, extensively drug-resistant, and incurable tuberculosis. *Lancet Respir Med* [online ahead of print] 15 Mar 2017; DOI: 10.1016/S2213-2600(17)30079-6.
3. Dheda K, Limberis JD, Pietersen E, Phelan J, Esmail A, Lesosky M, *et al*. Outcomes, infectiousness, and transmission dynamics of patients with extensively drug-resistant tuberculosis and home-discharged patients with programmatically incurable tuberculosis: a prospective cohort study. *Lancet Respir Med* 2017;5:269–281.
4. Dheda K, Gumbo T, Gandhi NR, Murray M, Theron G, Udwadia Z, *et al*. Global control of tuberculosis: from extensively drug-resistant to untreatable tuberculosis. *Lancet Respir Med* 2014;2:321–338.
5. Pietersen E, Ignatius E, Streicher EM, Mastrapa B, Padanilam X, Pooran A, *et al*. Long-term outcomes of patients with extensively drug-resistant tuberculosis in South Africa: a cohort study. *Lancet* 2014;383:1230–1239.
6. O'Donnell MR, Jarand J, Loveday M, Padayatchi N, Zelnick J, Werner L, *et al*. High incidence of hospital admissions with multidrug-resistant and extensively drug-resistant tuberculosis among South African health care workers. *Ann Intern Med* 2010;153:516–522.
7. McMillen CW. Discovering tuberculosis: a global history, 1900 to the present. New Haven and London: Yale University Press; 2015.
8. PREVENTION of streptomycin resistance by combined chemotherapy: a Medical Research Council investigation. *BMJ* 1952;1:1157–1162.
9. Selkon JB, Devadatta S, Kulkarni KG, Mitchison DA, Narayana AS, Nair CN, *et al*. The emergence of isoniazid-resistant cultures in patients with pulmonary tuberculosis during treatment with isoniazid alone or isoniazid plus PAS. *Bull World Health Organ* 1964;31:273–294.
10. Kempker RR, Kipiani M, Mirtskhulava V, Tukvadze N, Magee MJ, Blumberg HM. Acquired drug resistance in *Mycobacterium tuberculosis* and poor outcomes among patients with multidrug-resistant tuberculosis. *Emerg Infect Dis* 2015;21:992–1001.
11. Cegielski JP, Dalton T, Yagui M, Wattanaamornkiet W, Volchenkov GV, Via LE, *et al*.; Global Preserving Effective TB Treatment Study (PETTS) Investigators. Extensive drug resistance acquired during treatment of multidrug-resistant tuberculosis. *Clin Infect Dis* 2014;59:1049–1063.
12. Frieden TR, Fujiwara PI, Washko RM, Hamburg MA. Tuberculosis in New York City--turning the tide. *N Engl J Med* 1995;333:229–233.
13. Mitchison DA. How drug resistance emerges as a result of poor compliance during short course chemotherapy for tuberculosis. *Int J Tuberc Lung Dis* 1998;2:10–15.
14. Pasipanodya JG, Gumbo T. A meta-analysis of self-administered vs directly observed therapy effect on microbiologic failure, relapse, and acquired drug resistance in tuberculosis patients. *Clin Infect Dis* 2013;57:21–31.
15. Pasipanodya JG, McIlleron H, Burger A, Wash PA, Smith P, Gumbo T. Serum drug concentrations predictive of pulmonary tuberculosis outcomes. *J Infect Dis* 2013;208:1464–1473.
16. Pasipanodya JG, Srivastava S, Gumbo T. Meta-analysis of clinical studies supports the pharmacokinetic variability hypothesis for acquired drug resistance and failure of antituberculosis therapy. *Clin Infect Dis* 2012;55:169–177.
17. Srivastava S, Pasipanodya JG, Meek C, Leff R, Gumbo T. Multidrug-resistant tuberculosis not due to noncompliance but to between-patient pharmacokinetic variability. *J Infect Dis* 2011;204:1951–1959.
18. Schmalstieg AM, Srivastava S, Belkaya S, Deshpande D, Meek C, Leff R, *et al*. The antibiotic resistance arrow of time: efflux pump induction is a general first step in the evolution of mycobacterial drug resistance. *Antimicrob Agents Chemother* 2012;56:4806–4815.
19. Kempker RR, Rabin AS, Nikolaishvili K, Kalandadze I, Gogishvili S, Blumberg HM, *et al*. Additional drug resistance in *Mycobacterium tuberculosis* isolates from resected cavities among patients with multidrug-resistant or extensively drug-resistant pulmonary tuberculosis. *Clin Infect Dis* 2012;54:e51–e54.
20. Driver ER, Ryan GJ, Hoff DR, Irwin SM, Basaraba RJ, Kramnik I, *et al*. Evaluation of a mouse model of necrotic granuloma formation using C3HeB/FeJ mice for testing of drugs against *Mycobacterium tuberculosis*. *Antimicrob Agents Chemother* 2012;56:3181–3195.
21. Prideaux B, Via LE, Zimmerman MD, Eum S, Sarathy J, O'Brien P, *et al*. The association between sterilizing activity and drug distribution into tuberculosis lesions. *Nat Med* 2015;21:1223–1227.
22. Kempker RR, Heinrichs MT, Nikolaishvili K, Sabulua I, Bablishvili N, Gogishvili S, *et al*. Lung tissue concentrations of pyrazinamide among patients with drug-resistant pulmonary tuberculosis. *Antimicrob Agents Chemother* 2017;61:e00226-17.
23. Moreno-Gamez S, Hill AL, Rosenbloom DI, Petrov DA, Nowak MA, Pennings PS. Imperfect drug penetration leads to spatial monotherapy and rapid evolution of multidrug resistance. *Proc Natl Acad Sci USA* 2015;112:E2874–E2883.
24. Chigutsa E, Pasipanodya JG, Visser ME, van Helden PD, Smith PJ, Sirgel FA, *et al*. Impact of nonlinear interactions of pharmacokinetics and MICs on sputum bacillary kill rates as a marker of sterilizing effect in tuberculosis. *Antimicrob Agents Chemother* 2015;59:38–45.
25. Gumbo T, Dona CS, Meek C, Leff R. Pharmacokinetics-pharmacodynamics of pyrazinamide in a novel in vitro model of tuberculosis for sterilizing effect: a paradigm for faster assessment of new antituberculosis drugs. *Antimicrob Agents Chemother* 2009;53:3197–3204.
26. Srivastava S, Musuka S, Sherman C, Meek C, Leff R, Gumbo T. Efflux-pump-derived multiple drug resistance to ethambutol monotherapy in *Mycobacterium tuberculosis* and the pharmacokinetics and pharmacodynamics of ethambutol. *J Infect Dis* 2010;201:1225–1231.
27. Gumbo T, Louie A, Liu W, Brown D, Ambrose PG, Bhavnani SM, *et al*. Isoniazid bactericidal activity and resistance emergence: integrating pharmacodynamics and pharmacogenomics to predict efficacy in different ethnic populations. *Antimicrob Agents Chemother* 2007;51:2329–2336.
28. Gumbo T, Louie A, Deziel MR, Liu W, Parsons LM, Salfinger M, *et al*. Concentration-dependent *Mycobacterium tuberculosis* killing and prevention of resistance by rifampin. *Antimicrob Agents Chemother* 2007;51:3781–3788.

29. Gumbo T, Louie A, Deziel MR, Parsons LM, Salfinger M, Drusano GL. Selection of a moxifloxacin dose that suppresses drug resistance in *Mycobacterium tuberculosis*, by use of an in vitro pharmacodynamic infection model and mathematical modeling. *J Infect Dis* 2004;190: 1642–1651.
30. Gumbo T, Pasipanodya JG, Wash P, Burger A, McIlleron H. Redefining multidrug-resistant tuberculosis based on clinical response to combination therapy. *Antimicrob Agents Chemother* 2014;58:6111–6115.
31. Srivastava S, Pasipanodya JG, Ramachandran G, Deshpande D, Shuford S, Crosswell HE, *et al*. A long-term co-perfused disseminated tuberculosis-3D liver hollow fiber model for both drug efficacy and hepatotoxicity in babies. *EBioMedicine* 2016;6:126–138.
32. Deshpande D, Srivastava S, Pasipanodya JG, Lee PS, Gumbo T. A novel ceftazidime/avibactam, rifabutin, tedizolid and moxifloxacin (CARTM) regimen for pulmonary *Mycobacterium avium* disease. *J Antimicrob Chemother* 2017;72:i48–i53.
33. Gumbo T, Pasipanodya JG, Romero K, Hanna D, Nuermberger E. Forecasting accuracy of the hollow fiber model of tuberculosis for clinical therapeutic outcomes. *Clin Infect Dis* 2015;61:S25–S31.
34. Court R, Wiesner L, Stewart A, de Vries N, Harding J, Maartens G, *et al*. Steady state pharmacokinetics of cycloserine in patients on terizidone for multidrug-resistant tuberculosis. *Int J Tuberc Lung Dis* 2018;22:30–33.
35. Alligood KT, Sauer TD, Yorke JA. Chaos: an introduction to dynamical systems. New York: Springer; 1996.
36. Gumbo T, Chigutsa E, Pasipanodya J, Visser M, van Helden PD, Sirgel FA, *et al*. The pyrazinamide susceptibility breakpoint above which combination therapy fails. *J Antimicrob Chemother* 2014;69:2420–2425.
37. Singh R. Determination of minimum inhibitory concentration of cycloserine in multidrug resistant M*ycobacterium tuberculosis* isolates. *Jordan J Biol Sci* 2014;7:139–145.
38. Schön T, Juréen P, Chryssanthou E, Giske CG, Sturegård E, Kahlmeter G, *et al*. Wild-type distributions of seven oral second-line drugs against *Mycobacterium tuberculosis*. *Int J Tuberc Lung Dis* 2011;15: 502–509.
39. Rockwood N, Pasipanodya JG, Denti P, Sirgel F, Lesosky M, Gumbo T, *et al*. Concentration-dependent antagonism and culture conversion in pulmonary tuberculosis. *Clin Infect Dis* 2017;64: 1350–1359.
40. Gumbo T, Angulo-Barturen I, Ferrer-Bazaga S. Pharmacokinetic-pharmacodynamic and dose-response relationships of antituberculosis drugs: recommendations and standards for industry and academia. *J Infect Dis* 2015;211:S96–S106.
41. Zheng X, Zheng R, Hu Y, Werngren J, Forsman LD, Mansjö M, *et al*. Determination of MIC breakpoints for second-line drugs associated with clinical outcomes in multidrug-resistant tuberculosis treatment in China. *Antimicrob Agents Chemother* 2016;60:4786–4792.
42. Gumbo T. New susceptibility breakpoints for first-line antituberculosis drugs based on antimicrobial pharmacokinetic/ pharmacodynamic science and population pharmacokinetic variability. *Antimicrob Agents Chemother* 2010;54:1484–1491.
43. Hol FJ, Hubert B, Dekker C, Keymer JE. Density-dependent adaptive resistance allows swimming bacteria to colonize an antibiotic gradient. *ISME J* 2016;10:30–38.
44. Baym M, Lieberman TD, Kelsic ED, Chait R, Gross R, Yelin I, *et al*. Spatiotemporal microbial evolution on antibiotic landscapes. *Science* 2016;353:1147–1151.
45. Akkerman OW, van Altena R, Klinkenberg T, Brouwers AH, Bongaerts AH, van der Werf TS, *et al*. Drug concentration in lung tissue in multidrug-resistant tuberculosis. *Eur Respir J* 2013;42: 1750–1752.
46. Wang Q, Pang Y, Jing W, Liu Y, Wang N, Yin H, *et al*. Clofazimine for treatment of extensively drug-resistant pulmonary tuberculosis in China. *Antimicrob Agents Chemother* 2018;62:e02149-17.
47. Lieberman TD, Wilson D, Misra R, Xiong LL, Moodley P, Cohen T, *et al*. Genomic diversity in autopsy samples reveals within-host dissemination of HIV-associated *Mycobacterium tuberculosis*. *Nat Med* 2016;22:1470–1474.